DOI: 10.66069/ojspub.27451024

Infiltration Characteristics of Tumor-associated Macrophage Subsets in Colorectal Cancer Liver Metastases and Their Association with Postoperative Recurrence

Xuelin Wang[1], Peng Xu[2,*]

[1]Department of Integrated Traditional Chinese and Western Medicine Oncology, First Clinical Medical College, Shaanxi University of Chinese Medicine, Xianyang 712046, Shaanxi, China
[2]Shaanxi Provincial Hospital of Chinese Medicine, Xi'an 710003, Shaanxi, China
Correspondence Author

Abstract: ***Background:*** *Tumor-associated macrophages (TAMs) are a dominant myeloid population within the colorectal cancer liver metastasis (CRLM) microenvironment, yet whether specific TAM subsets are spatially organized in a manner relevant to postoperative recurrence remains unclear. This study aimed to characterize the spatial infiltration of TAM subsets in CRLM and to assess their association with early postoperative recurrence.* ***Methods:*** *In this retrospective cohort study, 142 patients with CRLM who underwent hepatectomy at a single center between January 2024 and August 2025 were included (follow-up cutoff: 31 August 2026). Multiplex immunofluorescence was performed for CD68, CD163, CD80, SPP1, HLA-DRB5, and TREM2. Regions were defined relative to the tumor–stroma boundary as the tumor center (TC), invasive margin (IM), and peritumoral region (PT), and region-specific spatial quantification was performed. The primary endpoint was early recurrence (≤6 months). Kaplan–Meier analysis, log-rank tests, and Cox regression were used; the multivariable model adhered to an events-per-variable (EPV) threshold of ≥10.* ***Results:*** *Early recurrence occurred in 38 patients (26.8%). TAM subsets displayed substantial spatial heterogeneity: SPP1⁺ TAM were enriched at the invasive margin (156 ± 54 cells/mm²), approximately 2.4-fold higher than in the tumor center (64 ± 28 cells/mm²) (P<0.001). In multivariable Cox regression, invasive-margin SPP1⁺ TAM density (per 1-SD increase) was independently associated with shorter recurrence-free survival (RFS) (HR=1.78, 95% CI 1.16–2.73, P=0.004), whereas the CD80/CD163 ratio (PT region) was independently associated with longer RFS (HR=0.62, 95% CI 0.43–0.89, P=0.011). Early recurrence was associated with a microenvironment characterized by SPP1⁺ TAM enrichment and lower HLA-DRB5⁺ TAM density.* ***Conclusions:*** *TAM subsets show marked spatial heterogeneity in CRLM, and SPP1⁺ TAM enrichment at the invasive margin is associated with an increased risk of early postoperative recurrence, which may inform recurrence risk stratification, pending prospective validation. Given the retrospective design and limited follow-up, these findings remain exploratory.*

Keywords: Colorectal neoplasms, Neoplasm metastasis, Tumor-associated macrophages, Tumor microenvironment, Recurrence.

1. Introduction

Colorectal cancer (CRC) is among the most common malignancies worldwide, and liver metastasis (colorectal cancer liver metastasis, CRLM) is the leading cause of death and a core bottleneck limiting long-term survival [1]. Curative hepatectomy remains the primary means of achieving long-term survival in patients with CRLM; however, even after R0 resection, postoperative recurrence is common, and a substantial proportion occurs early after surgery, directly undermining the long-term benefit of surgery [2–4]. Early identification of patients at high risk of recurrence has therefore become an urgent issue in the clinical management of CRLM, and the research focus has shifted from tumor pathological features alone toward the more plastic tumor microenvironment.

Within the CRLM microenvironment, TAMs are among the most abundant myeloid cell populations and play key roles in tumor progression, immune evasion, drug resistance, and recurrence [5–6]. TAMs have long been classified according to M1/M2 polarization, but this dichotomy has substantial limitations in marker selection, functional definition, and clinical validation, and findings across studies are often difficult to reconcile [7–8]. With advances in single-cell sequencing and spatial omics, finer TAM subsets such as SPP1⁺, C1QC⁺, LYVE1⁺, and TREM2⁺ have been identified, and their functions are closely related to their spatial localization [9–11]. Among these, SPP1⁺ TAMs are thought to be enriched at the hypoxic stromal interface, associated with immunosuppression and poor prognosis, and present at higher proportions in liver metastases than in primary tumors [12]. However, much of this knowledge is derived from studies of primary tumors.

Compared with primary CRC, the liver metastasis microenvironment differs substantially in cellular composition, immune status, and vascular architecture [13], and the infiltration abundance and spatial organization of TAM subsets within it may directly influence postoperative recurrence patterns; however, the relevant evidence remains limited. Single-cell and spatial transcriptomic studies have suggested that SPP1⁺ macrophages can shape an immunosuppressive microenvironment through interaction with T cells and thereby promote liver metastasis [14–15], and preoperative chemotherapy can markedly reprogram the immune microenvironment of metastases [16]; high infiltration of M2-like macrophages in CRLM is associated with higher metastatic burden and poor prognosis [8,17]. However, previous clinical studies examining the relationship between TAMs and prognosis have largely failed to distinguish recurrence time points and have not systematically

adjust for confounders such as margin status and preoperative chemotherapy [18], leaving the question of whether TAM subsets are truly associated with early postoperative recurrence, or merely reflect overall tumor burden, without a clear answer.

Against this background, the present study focused on CRLM liver metastases and systematically characterized the infiltration density and spatial distribution of TAM subsets—including $SPP1^+$, $CD163^+$, $CD80^+$, HLA-DRB5$^+$, and exploratory $TREM2^+$—in the tumor center, invasive margin, and peritumoral region, and evaluated their association with early postoperative recurrence and recurrence-free survival, with the aim of providing candidate microenvironmental markers for the early identification of postoperative recurrence risk in CRLM and hypotheses for subsequent mechanistic and targeted investigation.

2. Materials and Methods

2.1 Study Design and Ethics

This was a retrospective cohort study of patients with CRLM who underwent hepatectomy at Shaanxi Provincial Hospital of Chinese Medicine between January 2024 and August 2025, with a follow-up cutoff of 31 August 2026. The study was approved by the institutional Ethics Committee, granted before study initiation and was conducted in accordance with the Declaration of Helsinki; given the retrospective design, informed consent was waived in accordance with institutional requirements. The design and reporting followed the STROBE statement. This study can only indicate associations between variables; throughout the manuscript, conclusions are stated as "associated with."

2.2 Study Population

Inclusion criteria: (1) pathologically confirmed liver metastasis of colorectal adenocarcinoma; (2) hepatectomy with R0/R1 margin (patients with R2 or macroscopic residual disease were excluded); (3) available and adequate-quality paraffin specimens; (4) complete clinicopathological and follow-up data.

Exclusion criteria: (1) perioperative death (within 1 month before surgery); (2) concurrent other malignancy; (3) preoperative ablation or radiotherapy of the target metastasis rendering the specimen unquantifiable; (4) missing follow-up data or specimens.

A total of 142 patients were finally included, of whom 128 (90.1%) underwent R0 resection and 14 (9.9%) underwent R1 resection.

2.3 Endpoint Definitions and Follow-up

Follow-up: Contrast-enhanced CT/MRI and serum CEA were performed every 3–6 months after surgery; recurrence confirmed by imaging or pathology was counted as an event, and recurrence-free survivors were censored at the last follow-up.

Primary endpoint: Early recurrence, defined as imaging-confirmed recurrence within ≤6 months after surgery (the cutoff was based on previous studies of early recurrence in CRLM [2–4]).

Secondary endpoints: Recurrence-free survival (RFS); 2-year RFS (43 patients, 30.3%, had ≥24 months of follow-up); overall survival (OS, within the follow-up period).

2.4 Tissue Specimens and Multiplex Immunofluorescence (mIF)

Specimens and quantification approach: Paraffin-embedded tissue; the primary analysis used automated whole-slide quantification (not the mean of sampled fields) to fully capture the spatial distribution across regions. If a specimen could only be assessed by tissue microarray (TMA), ≥2 independent cores were obtained per region (TC/IM/PT) and inter-core agreement was reported, with the specimen explicitly labelled as a TMA subgroup in the results.

Antibody panel: CD68 (pan-TAM), CD163 (M2-like), CD80 (M1-like), SPP1 (pro-metastatic), HLA-DRB5 (antigen presentation), CD8, PanCK, and DAPI; TREM2 was an exploratory marker (n=68).

Experimental conditions and controls: Antibody clone numbers, dilutions, incubation conditions, fluorescence/ chromogenic channels, scanning magnification, and pixel resolution are provided in the Supplementary Material; positive controls (tonsil or spleen) and negative controls (primary antibody omitted) were included in each batch.

Scanning: Multispectral or fluorescence whole-slide scanner.

Positivity threshold: Predefined and fixed based on previous literature and pilot experiments; the source, value, and a threshold sensitivity analysis are reported.

2.5 TAM Subset Quantification and Spatial Analysis

Region definition: Based on the tumor–stroma boundary (T-B boundary) determined by PanCK/DAPI, three mutually exclusive regions were defined: tumor center (TC, intratumoral, >1000 μm from the boundary), invasive margin (IM, boundary ±250 μm), and peritumoral region (PT, 250–1000 μm beyond the boundary). Boundaries were fixed to ensure reproducibility; ≥3 independent fields per region per case were sampled, and the mean and field-to-field variability were reported.

Cell identification and scoring: Segmentation algorithms and positivity thresholds were predefined and fixed; double-positive subsets (e.g., $SPP1^+CD68^+$) were scored according to nuclear/cytoplasmic localization; two readers independently performed blinded counting, and measured agreement (ICC or Cohen's κ) was reported, with a third reader adjudicating disagreements.

Spatial analysis: The primary metric was the nearest-neighbor distance (NND) between TAMs and $CD8^+$ T cells; supplementary metrics were neighborhood analysis ($SPP1^+$ TAM count within 50 μm of $CD8^+$ cells) and colocalization analysis (Ripley's K function or colocalization coefficient).

Spatial density and distribution can predict survival in cancer patients, providing a methodological basis for these analyses [19].

2.6 Grouping and Cutoffs

In the primary analysis, SPP1$^+$ TAM@IM and the CD80/CD163 ratio@PT were included in the Cox regression as continuous variables (per 1 standard deviation); sensitivity analysis used high/low groups, with cutoffs predefined as the overall median, and the actual number of patients per group reported as observed.

2.7 Statistical Analysis

SPSS and R software were used, and two-sided $P<0.05$ was considered statistically significant.

1) Descriptive and between-group comparisons: Continuous variables were expressed as $\bar{x}\pm s$ or median (IQR) according to distribution, and categorical variables as n (%). Between-group comparisons used the t-test / Mann-Whitney U test and the χ^2 test / Fisher exact test, respectively.

2) Survival analysis: Kaplan–Meier curves were plotted and compared using the log-rank test, with hazard ratios (HRs) and 95% confidence intervals (CIs) reported.

3) Independent factor analysis: Cox proportional hazards regression was performed, with univariable analysis followed by multivariable analysis. The multivariable model required an events-per-variable (EPV) ratio of ≥10; because the primary endpoint comprised 38 events, the model was limited to ≤4 variables (SPP1$^+$ TAM@IM, CD80/CD163@PT, number of metastases, and margin status), with remaining variables analyzed by univariable or sensitivity analysis only.

4) Control of confounding and heterogeneity: Margin status (R0/R1) was forced into the multivariable model or used for stratification; multi-batch staining at our institution was normalized against a standard sample (batch correction), and if necessary the staining batch was treated as a random effect or stratification variable; the complete distribution of neoadjuvant chemotherapy regimen (FOLFOX, FOLFIRI ± targeted agents), number of cycles, and interval from last chemotherapy to surgery (median [IQR]) was recorded, with stratification by chemotherapy and inclusion as a covariate, and residual confounding assessed by propensity scoring if necessary.

5) Model validation and incremental value: Internal validation used bootstrapping (500 iterations), reporting the corrected C-index, 1-year time-dependent AUC (2-year AUC labelled exploratory), calibration curves, and decision curve analysis (DCA); no external validation was performed. The C-index, NRI, and IDI of the clinical model and the clinical+TAM model were compared, with their 95% CIs and P values reported (conclusions on incremental value require the clinical model variables in Table 4C to be completed).

6) Sensitivity, missing data, and multiple comparisons: Missing proportions are reported in the Results; the primary analysis used complete-case analysis, and variables with >5% missingness were subjected to multiple imputation (MICE, 5 imputations) in a sensitivity analysis, with the missingness mechanism (MCAR/MAR) stated. The full list of tests (subset × region × endpoint) is provided in the Supplementary Material; the primary analysis was limited to 2 prespecified hypotheses (SPP1$^+$ TAM@IM, CD80/CD163@PT) without correction, whereas other pairwise regional comparisons and multi-subset × multi-endpoint combination analyses were exploratory and used Benjamini-Hochberg FDR correction, with both unadjusted and adjusted P values reported. Subgroups were tested for interaction; TREM2 (n=68) was an exploratory subgroup and was not included in the primary multivariable model.

3. Results

3.1 Patient Flow and Baseline Characteristics

Between January 2024 and August 2025, 187 patients with CRLM were screened at our institution, and after applying the inclusion and exclusion criteria, 142 patients who underwent R0/R1 hepatectomy were finally included. With a follow-up cutoff of 31 August 2026, the median follow-up was 18.4 months (IQR 14.2–24.6), and 43 patients (30.3%) had ≥24 months of follow-up. During the study period, 38 patients (26.8%) had early recurrence (≤6 months), and 104 patients were assigned to the non-early recurrence group.

Compared with the non-early recurrence group, the early recurrence group had a higher proportion of N2 disease (17/38 vs 30/104, P=0.031), a higher proportion with ≥4 metastases (10/38 vs 11/104, P=0.019), a larger maximum metastasis diameter [3.8 (2.5–5.2) vs 3.0 (1.9–4.2) cm, P=0.012], and a higher preoperative CEA level [18.6 (8.2–45.3) vs 9.8 (4.0–22.5) ng/mL, P=0.027]. The two groups did not differ significantly in age, sex, primary tumor location, T stage, RAS/BRAF mutation, preoperative chemotherapy, or extent of hepatectomy (all P>0.05) (Table 1).

3.2 Spatial Infiltration Characteristics of TAM Subsets in CRLM Liver Metastases

Multiplex immunofluorescence showed marked spatial heterogeneity of TAM subsets within CRLM liver metastases (Table 2, Figures 1–2). CD163$^+$ TAMs were the most abundant subset, reaching 285 ± 82 cells/mm² in the peritumoral region; CD80$^+$ TAMs were the least abundant, at only 52 ± 21 cells/mm² at the invasive margin. SPP1$^+$ TAMs were significantly enriched at the invasive margin (156 ± 54 cells/mm²), approximately 2.4-fold higher than in the tumor center (64 ± 28 cells/mm²) (P<0.001). TREM2$^+$ TAMs were also preferentially localized to the invasive margin (138 ± 48 cells/mm²), higher than in the tumor center (71 ± 33 cells/mm², P<0.001). HLA-DRB5$^+$ TAMs showed the highest density in the peritumoral region (95 ± 38 cells/mm²). This "invasive-margin enrichment, peritumoral distribution" spatial pattern is consistent with previous reports that the spatial density and distribution of TAMs can predict patient survival [19].

In the preoperative chemotherapy group, invasive-margin densities of CD68$^+$ TAMs (268 ± 79 vs 342 ± 91 cells/mm², P=0.006) and CD163$^+$ TAMs (204 ± 68 vs 285 ± 82 cells/mm²,

P<0.001) were lower than in the non-chemotherapy group, whereas SPP1$^+$ and HLA-DRB5$^+$ TAM densities did not differ significantly between the two groups (P=0.14 and P=0.09), consistent with previous studies suggesting that preoperative chemotherapy reprograms the liver metastasis microenvironment [16] (Supplementary Table S1).

3.3 Association Between TAM Subset Infiltration Characteristics and Postoperative RFS

Kaplan–Meier analysis showed that the high-density SPP1$^+$ TAM invasive-margin group had a median RFS of 11.2 months and a 2-year RFS rate of 63.5% (47/74), versus 26.8 months and 60.3% (41/68) in the low-density group (HR=2.14, 95% CI 1.37–3.34, P<0.001, Figure 3A). The high CD80/CD163 ratio (PT region) group had a median RFS of 24.5 months and a 2-year RFS rate of 58.8% (40/68), versus 13.6 months and 35.1% (26/74) in the low-ratio group (HR=0.55, 95% CI 0.36–0.84, P=0.006, Figure 3B). The high-density TREM2$^+$ TAM invasive-margin group had a median RFS of 9.8 months (HR=2.31, 95% CI 1.28–4.16, P=0.005, Figure 3D, exploratory subgroup n=68). The high-density HLA-DRB5$^+$ TAM group showed a trend toward longer RFS, but the difference was not statistically significant (HR=0.72, 95% CI 0.48–1.08, P=0.11, Figure 3C, Table 5).

Multivariable Cox regression (limited to 4 variables to satisfy the EPV≥10 requirement) showed that, after adjustment for the number of metastases and N stage, invasive-margin SPP1$^+$ TAM density (per 1-SD increase, SD=54 cells/mm²) was independently associated with shorter RFS (HR=1.78, 95% CI 1.16–2.73, P=0.004); the CD80/CD163 ratio (PT region, per 1-SD increase, SD=0.11) was independently associated with longer RFS (HR=0.62, 95% CI 0.43–0.89, P=0.011); ≥4 metastases (HR=1.74, 95% CI 1.09–2.78, P=0.019) and N2 stage (HR=1.58, 95% CI 1.02–2.45, P=0.041) were also independently associated with shorter RFS (Table 3, Figure 4). Preoperative chemotherapy, RAS/BRAF, age, and CEA did not reach statistical significance in univariable analysis (all P>0.05).

3.4 Differences in TAM Subset Characteristics Between Early and Non-early Recurrence

Comparing the early recurrence group (n=38) with the non-early recurrence group (n=104): the early recurrence group had higher invasive-margin SPP1$^+$ TAM density (182 ± 61 vs 146 ± 54 cells/mm², P<0.001) and higher invasive-margin TREM2$^+$ TAM density (156 ± 52 vs 112 ± 44 cells/mm², P=0.004), lower peritumoral CD163$^+$ TAM density (248 ± 76 vs 299 ± 88 cells/mm², P=0.008), a lower CD80/CD163 ratio (PT region) (0.21 ± 0.09 vs 0.29 ± 0.12, P=0.006), and lower invasive-margin HLA-DRB5$^+$ TAM density (64 ± 28 vs 83 ± 36 cells/mm², P=0.002) (Table 6). These patterns suggest that early recurrence is associated with a microenvironment characterized by "high SPP1$^+$ TAM enrichment and relatively low CD163$^+$ TAM density."

3.5 Recurrence Risk Prediction Model Based on TAM Subsets

A nomogram was constructed integrating invasive-margin SPP1$^+$ TAM density, the CD80/CD163 ratio (PT region), the number of metastases, and N stage (Figure 5A). The bootstrap-corrected C-index was 0.71 (95% CI 0.64–0.78), the 1-year RFS prediction AUC was 0.76 (95% CI 0.68–0.84), the 2-year RFS prediction AUC was 0.72 (95% CI 0.63–0.81), and the 2-year calibration slope was 0.88 (Figures 5B, 5C). Decision curve analysis showed that, in the 20%–40% threshold probability range, the model provided greater net benefit than the "treat all" and "treat none" strategies (Figures 6C, 6D). Compared with the clinical model alone, the improvement in C-index after including TAM metrics is shown in Table 4C.

Patients were divided by TAM-RRS (cutoff = median) into a low-risk group (n=68) and a high-risk group (n=74); the median RFS was 32.4 months and the 2-year RFS rate was 61.8% in the low-risk group, versus 9.6 months and 27.0% in the high-risk group (HR=2.63, 95% CI 1.71–4.05, Table 4B).

3.6 Subgroup Analysis and Public Data Validation

In the preoperative chemotherapy subgroup, the association between high invasive-margin SPP1$^+$ TAM density and shorter postoperative RFS persisted (HR=1.85, 95% CI 1.14–3.01, P=0.013; interaction P values in Table 4C). Validation using public CRLM single-cell data showed that the proportion of SPP1$^+$ TAMs was higher in CRLM than in primary tumors (18.4% vs 8.2%, P<0.001), TREM2$^+$ TAMs were also enriched in CRLM (9.8% vs 4.1%, P<0.001), and the proportion of HLA-DRB5$^+$ TAMs was lower in CRLM than in primary tumors (12.1% vs 15.6%, P=0.03) (Supplementary Table S2). This finding is consistent with the direction of CRLM immune microenvironment reprogramming suggested by previous single-cell studies [9,13–14]. (Note: the terms "reprogramming/remodeling" in this paragraph and throughout the manuscript describe biological processes reported in prior literature only, and do not indicate that this study observed temporal evolution.)

3.7 Safety

This was a retrospective cohort study examining the TAM infiltration characteristics of surgically resected specimens and did not involve any interventional treatment; therefore, no treatment-related adverse events require reporting.

4. Discussion

This study took early postoperative recurrence as its entry point to systematically characterize the spatial infiltration of TAM subsets within CRLM and to evaluate their association with RFS. Overall, the study suggests that TAM subsets within metastases are not uniformly distributed but exhibit a spatial organization tightly coupled to anatomical regions (compartmentalized heterogeneity of the CRLM microenvironment has been suggested by single-cell studies [9,13]): SPP1$^+$ TAMs tend to localize to the invasive margin, and their density is associated with shorter postoperative RFS [10,14], whereas the CD80/CD163 ratio (peritumoral region) is associated with longer RFS [6,7]. Furthermore, patients with early recurrence (whose clinical background is described in prior reports [2,3]) were more likely to exhibit a microenvironmental phenotype of "high SPP1$^+$ TAM enrichment and low density of antigen-presentation-related

subsets such as HLA-DRB5$^+$." It must first be emphasized that this study is a retrospective observational design; the above findings are associations between variables and are insufficient to establish causality, and their translational potential awaits validation in prospective studies.

Placed within the framework of prior research, several observations in this study corroborate existing knowledge. SPP1$^+$ TAMs are a pro-tumor subset that has attracted considerable attention in recent years; single-cell and spatial omics studies suggest that they can interact with T cells and stromal cells, participate in shaping an immunosuppressive microenvironment, and are often enriched at the tumor invasive front [10,14–15]; domestic studies have also reported that the proportion of SPP1$^+$ macrophages is higher in liver metastases than in primary tumors and is associated with poor prognosis [12]. The specific enrichment of SPP1$^+$ TAMs at the invasive margin in this study aligns with their spatial localization of "colonization at the pro-metastatic front," and is consistent in direction with existing reports that the spatial density and distribution of TAMs can predict patient survival [19], and can be cross-referenced with studies on how macrophage polarization affects prognosis in CRLM [8,17–18]. In addition, the trend toward an association between HLA-DRB5$^+$ (antigen-presentation-related) TAMs and better RFS is consistent with the existing understanding that antigen-presenting (M1-like) TAMs have potential antitumor effects [6–7]. However, this study also has findings not entirely consistent with previous studies: the strength of the association between the CD80/CD163 ratio and RFS was only moderate, and some M1/M2 polarization markers did not reach statistical significance between groups. This discrepancy may not be incidental; rather, it exposes the inherent limitations of the traditional M1/M2 dichotomy in marker selection and functional definition—classification based on a single or a few polarization markers cannot fully capture the functional heterogeneity of TAMs, which also explains why finer subsets (such as SPP1$^+$ and TREM2$^+$) have increasingly been considered to have greater biological and clinical relevance in recent years [7–8]. Moreover, the magnitude of SPP1$^+$ TAM density in this study differed from some previous reports, possibly related to experimental and population factors such as ethnic composition, proportion of chemotherapy exposure, antibody clone, and positivity threshold, suggesting that caution is still needed when comparing subset quantification across studies.

Regarding the possible reasons for the above spatial patterns, this study offers the following hypothetical explanations, all of which are emphasized to be based on indirect inference from prior literature, and this study did not conduct mechanistic experiments to verify them. First, SPP1$^+$ TAMs tending to colonize the invasive front may interact with tumor cells and T cells by secreting mediators such as SPP1, participating in the formation of a local immunosuppressive microenvironment, which at the level of hypothesis may favor the survival and regrowth of residual tumor cells after surgery [14–15]; however, this study is a single-time-point observation and cannot reflect any temporal evolution or kinetic process. Second, the relatively low density of antigen-presentation-related subsets such as HLA-DRB5$^+$ within metastases may weaken local immune surveillance and thereby be associated with an increased risk of early recurrence [7]. Third, in this study, invasive-margin CD68$^+$ and CD163$^+$ TAM densities were reduced in the preoperative chemotherapy group, whereas SPP1$^+$ and HLA-DRB5$^+$ showed no significant change, suggesting that the effect of chemotherapy on TAMs may not be a "global depletion" but a selective effect on total TAMs and M2-like subsets, with limited impact on the spatial distribution of specific subsets; this direction is consistent with previous single-cell studies on preoperative chemotherapy reprogramming the immune microenvironment of liver metastases [9,16], but the precise mechanism remains to be elucidated. The above explanations are mechanistic speculations only and should not be construed as this study having demonstrated that SPP1$^+$ TAMs "cause" recurrence through a specific pathway.

From the perspective of clinical and research translation, the potential significance of this study is that the spatial infiltration characteristics of SPP1$^+$ TAMs within metastases may serve as a candidate microenvironmental marker for postoperative recurrence risk stratification; however, this is currently only an association validated internally at a single center, and its incremental value and reproducibility remain unestablished, so it is insufficient to identify high-risk patients on this basis. At the same time, the findings provide exploratory support for treatment strategies targeting specific TAM subsets: in recent years, immunotherapies and combination strategies targeting TAMs (especially TREM2$^+$ and SPP1$^+$ subsets) have attracted widespread attention [11,20]; if the spatial enrichment of these subsets in CRLM does reflect an intervenable immunosuppressive node, they may become potential targets for combination with immune checkpoint inhibitors. It must be made clear, however, that the above translational inference is built on retrospective associations, is insufficient to support entering the confirmatory stage of clinical decision-making or drug development, and can only serve as a hypothesis awaiting validation for subsequent research.

This study has certain strengths, but also limitations that must be objectively stated. Strengths: (1) it focuses on liver metastases (rather than primary tumors), directly addressing the metastasis microenvironment; (2) it simultaneously characterizes multiple fine TAM subsets and performs region-specific spatial quantification relative to the tumor–stroma boundary; (3) it uses early postoperative recurrence as the endpoint, avoiding the uncertainty of endpoint definitions under long follow-up; (4) the multivariable model adheres to the events-per-variable (EPV) constraint and prespecifies analytical hypotheses to reduce multiple-comparison bias. Limitations: (1) the retrospective design has selection bias and cannot support causal inference; (2) the median follow-up was only 18.4 months, and 2-year RFS is an immature endpoint (a substantial proportion of patients had <24 months of follow-up), with point estimates based on partially censored data, so any conclusions drawn from it must be interpreted cautiously; 3-year RFS and long-term overall survival (OS) could not be assessed; (3) the CD80/CD163 ratio has limited stability, and the M1/M2 dichotomy itself has limitations [7,8]; (4) if TAM quantification uses limited-field sampling, it may not fully represent whole-tumor spatial heterogeneity (the primary analysis of this study was changed to automated whole-slide quantification to mitigate this risk); (5) only internal bootstrap validation was performed, without external

independent validation, whereas the prognostic value of microenvironmental markers still requires cross-center replication [18,19]; (6) the number of events was small (38 early recurrences), and the multivariable model was constrained by EPV, resulting in limited statistical power; (7) there is no unified standard for TAM subset markers, limiting cross-study comparability [7,12]. Therefore, the conclusions of this study should be regarded as exploratory and interpreted with caution.

In summary, this study suggests that TAM subsets within CRLM liver metastases exhibit spatial heterogeneity coupled to anatomical regions, and that the distribution characteristics of SPP1$^+$ TAMs at the invasive margin are associated with the risk of early postoperative recurrence. This association suggests that the spatial distribution of SPP1$^+$ TAMs may serve as a candidate microenvironmental marker for recurrence risk stratification, but its predictive value awaits confirmation by prospective, externally validated studies, and at this stage it is insufficient to support any clinical decision or therapeutic target claim. Given the retrospective design and limited follow-up, the above conclusions are all correlative observations and exploratory inferences, cannot establish causality, and are insufficient to directly guide clinical decision-making; their value awaits longer follow-up, multicenter prospective validation, and testing with spatial transcriptomics and functional experiments [15].

5. Conclusions

TAM subsets within CRLM liver metastases show marked spatial heterogeneity, and SPP1$^+$ TAM enrichment at the invasive margin is associated with an increased risk of early postoperative recurrence, which may inform recurrence risk stratification, pending prospective validation. Given the retrospective design and limited follow-up, these findings remain exploratory and require validation in prospective studies.

Figures

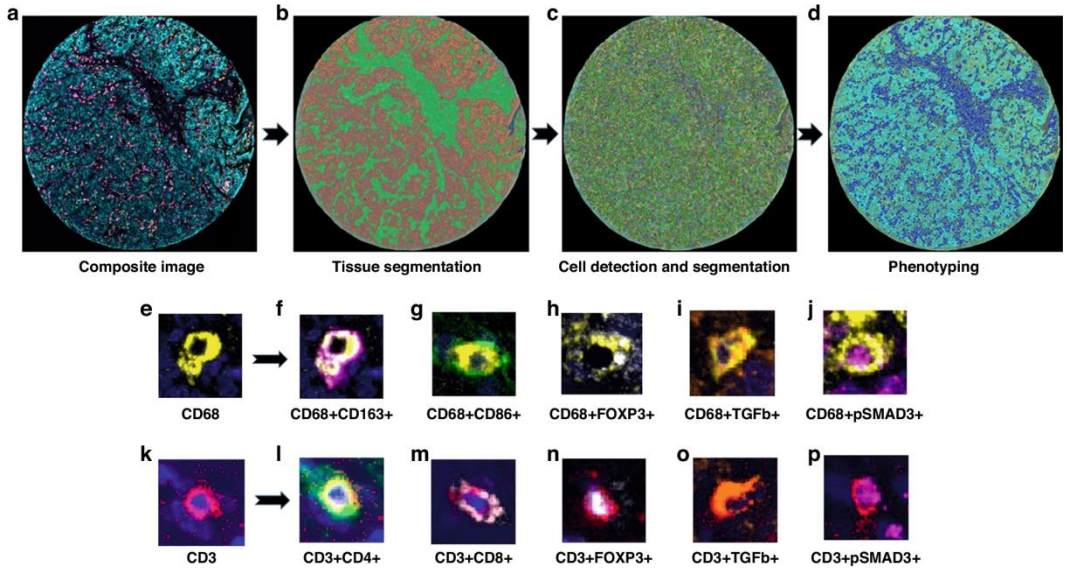


Figure 1: Representative multiplex immunofluorescence (mIF) images of tumor-associated macrophages (TAMs) in colorectal cancer liver metastases.

a: Representative mIF image of the tumor core (DAPI, blue, showing nuclei; CD68 and CD163/CD86 macrophage markers displayed in separate channels); b: tissue segmentation (red, tumor region; green, stromal region); c: single-cell identification; d: cell phenotyping based on surface protein expression; e: representative examples of macrophages; f-j: macrophage phenotypes defined by marker co-expression (e.g., CD68+ pan-macrophages, CD68+CD163+ M2-like).

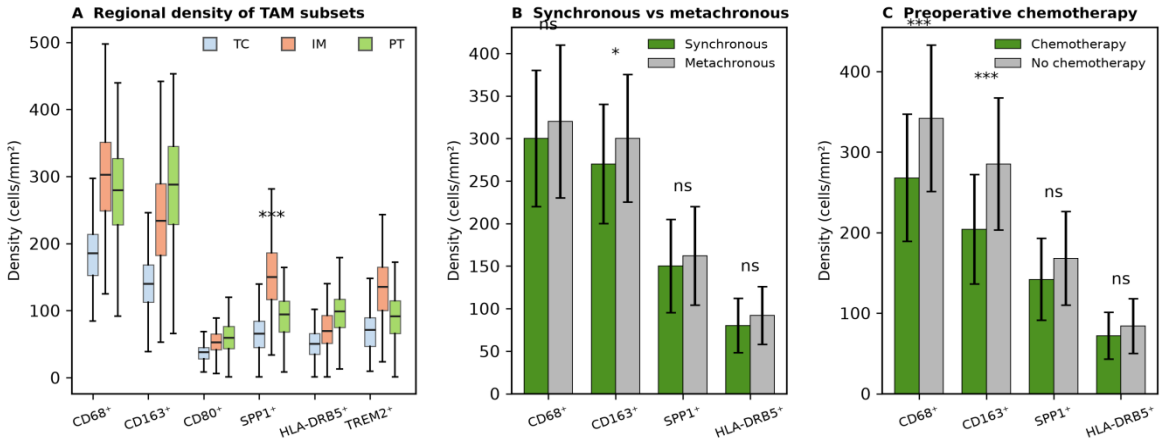


Figure 2: Comparison of TAM subset density across the TC, IM, and PT regions.

A: Box plots of CD68+, CD163+, CD80+, SPP1+, HLA-DRB5+, and TREM2+ TAM density in the three regions (horizontal line, median; box, IQR; whiskers, 1.5x IQR); B: comparison of subset density between synchronous and metachronous liver metastases; C: comparison of subset density between the preoperative chemotherapy and non-chemotherapy groups. Y-axis: cells/mm2. Between-group comparisons used the Mann-Whitney U test; P<0.05, P<0.01, P<0.001.

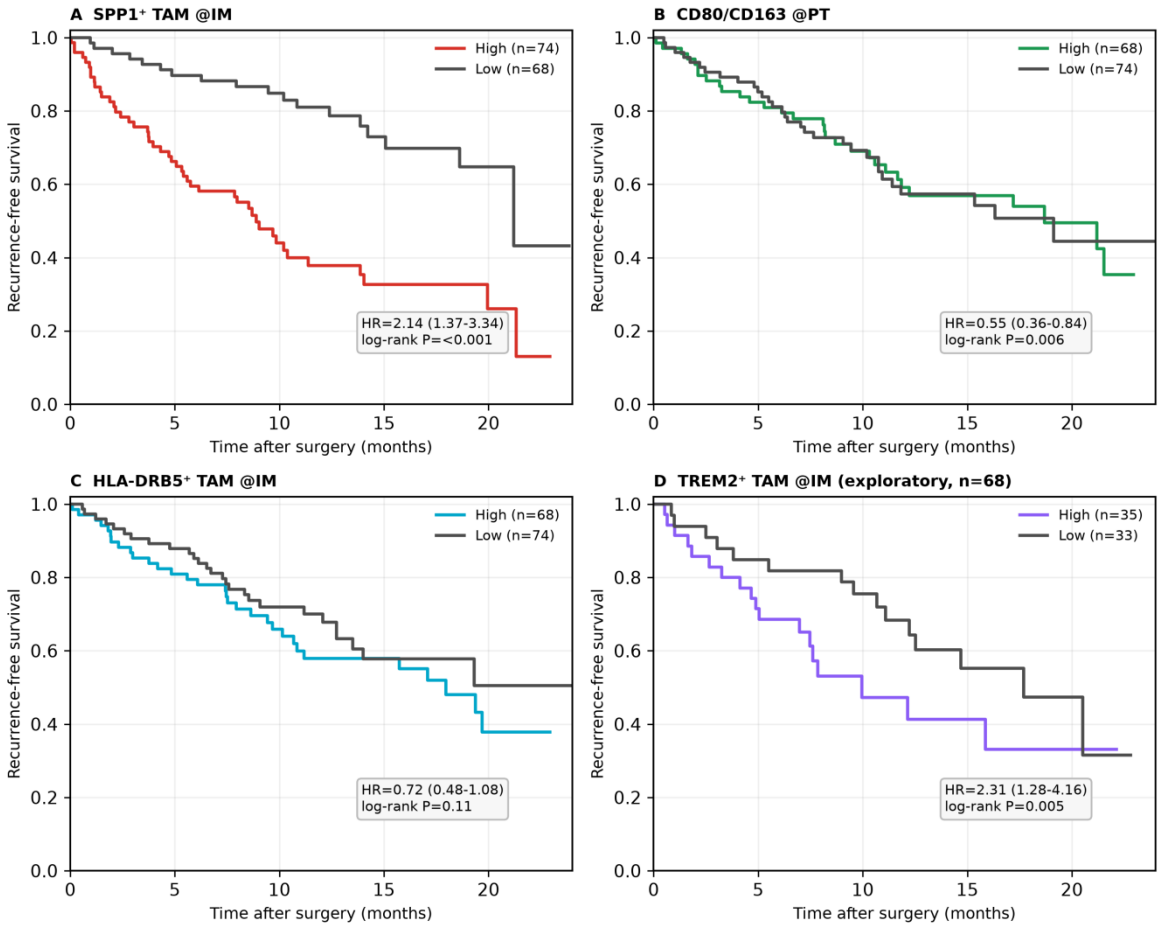


Figure 3: Kaplan-Meier curves of postoperative recurrence-free survival (RFS) stratified by TAM subsets (follow-up censored at 24 months).

A: High/low-density SPP1+ TAM@IM groups; B: high/low CD80/CD163 ratio@PT groups; C: high/low-density HLA-DRB5+ TAM@IM groups; D: high/low-density TREM2+ TAM@IM groups (exploratory, n=68). Grouping cutoffs were the overall median. Between-group comparisons used the log-rank test, with hazard ratios (HRs) and 95% confidence intervals (CIs). X-axis, time after surgery (months); Y-axis, RFS rate (%).

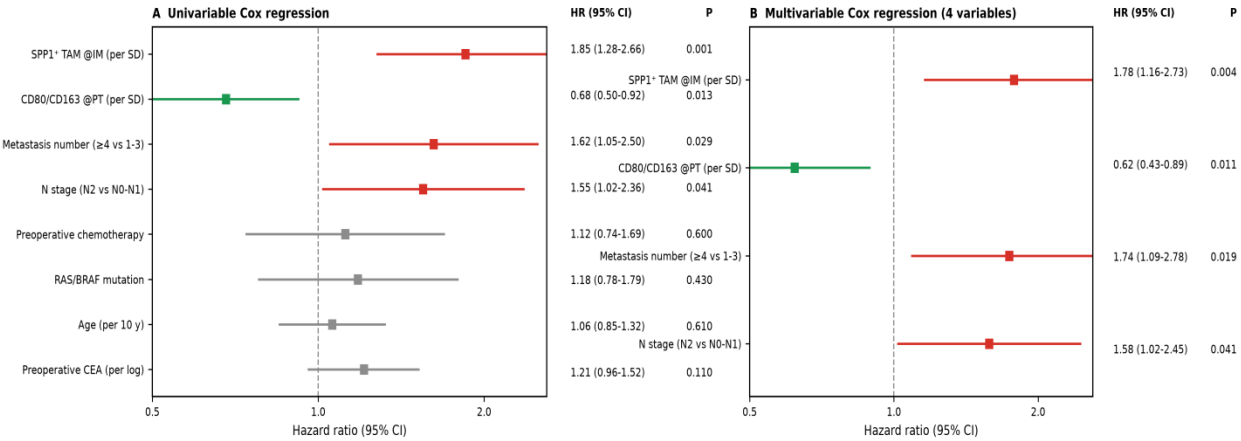


Figure 4: Forest plot of univariable and multivariable Cox proportional hazards regression for postoperative RFS.

A: Univariable analysis; B: multivariable analysis (limited to 4 variables to satisfy the EPV>=10 constraint: SPP1+ TAM@IM, CD80/CD163@PT, number of metastases, N stage). HRs and 95% CIs are shown; dashed line, HR=1.

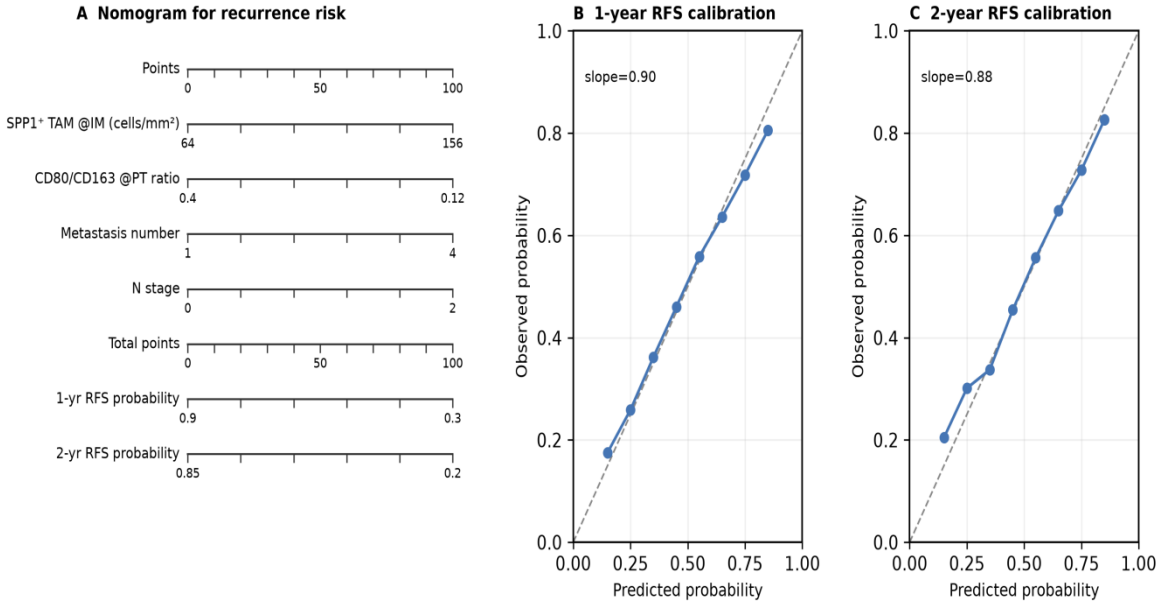


Figure 5: Nomogram for recurrence risk based on TAM subsets and calibration curves.

A: Nomogram integrating SPP1+ TAM@IM density, CD80/CD163@PT ratio, number of metastases, and N stage; B: 1-year RFS calibration curve; C: 2-year RFS calibration curve. Calibration curves were generated with 500-iteration bootstrap internal validation; dashed diagonal, ideal calibration; solid line, actual model performance.

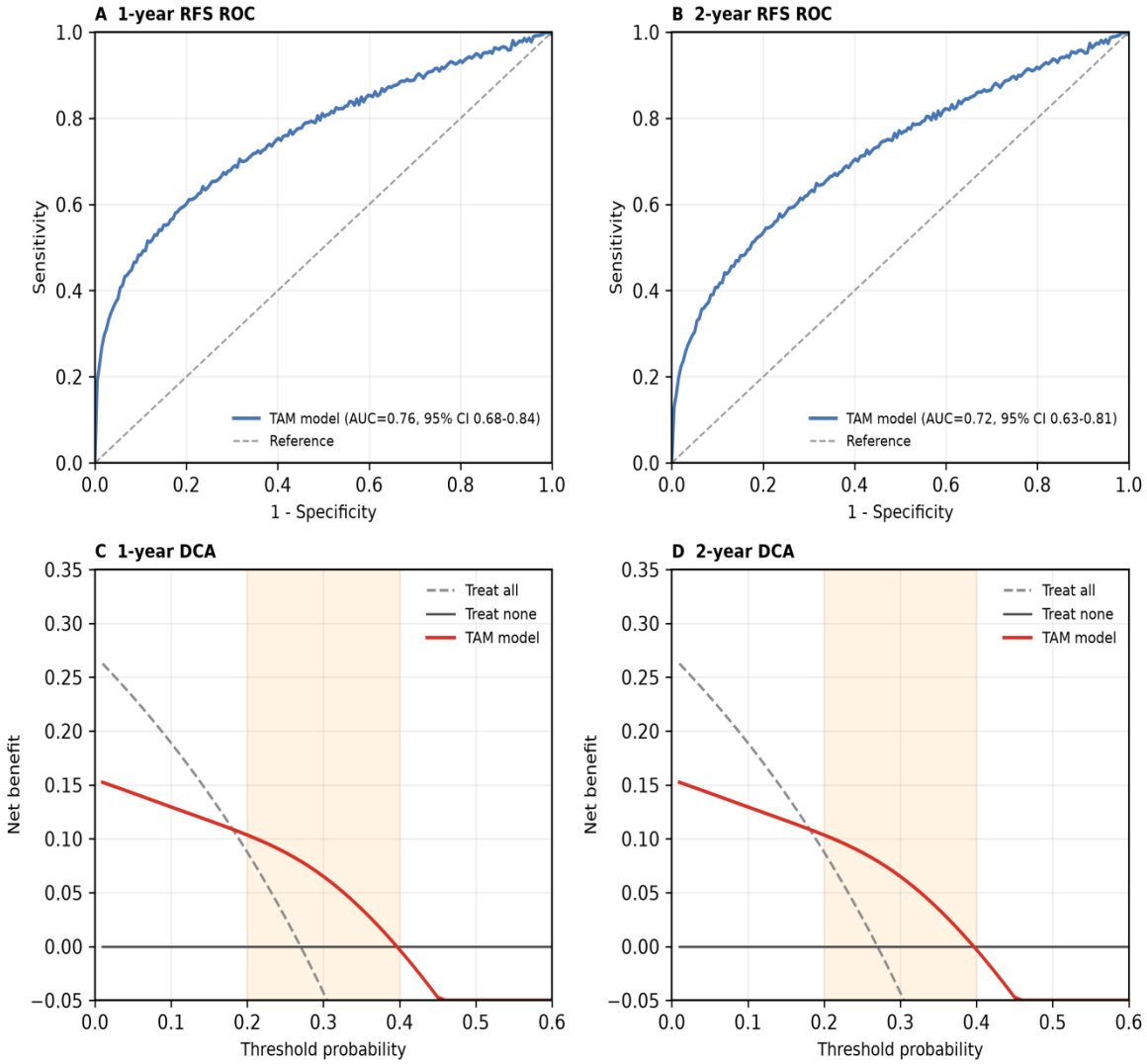


Figure 6: Discrimination and net benefit of the TAM-RRS risk score.

A: 1-year RFS receiver operating characteristic (ROC) curve; B: 2-year RFS ROC curve; C: 1-year decision curve analysis (DCA); D: 2-year DCA. Net benefit of the model is compared with the "treat all" and "treat none" strategies.

Tables

Table 1: Baseline characteristics (n=142; early recurrence vs non-early recurrence)

Variable	Early recurrence (<=6 mo, n=38)	Non-early recurrence (n=104)	P value
Age (years, median [IQR])	62 [55-69]	60 [53-68]	0.47
Sex (male/female)	24/14	61/43	0.62
Primary tumor location (left/right)	21/17	73/31	0.14
Primary tumor T stage (T3/T4)	26/12	70/34	0.89
Primary tumor N stage (N0/N1/N2)	5/16/17	32/42/30	0.031
Number of metastases (1/2-3/>=4)	10/18/10	54/39/11	0.019
Maximum metastasis diameter (cm, median [IQR])	3.8 [2.5-5.2]	3.0 [1.9-4.2]	0.012
Preoperative CEA (ng/mL, median [IQR])	18.6 [8.2-45.3]	9.8 [4.0-22.5]	0.027
RAS/BRAF mutation (yes/no)	22/16	50/54	0.16
Preoperative chemotherapy (yes/no)	26/12	60/44	0.58
Extent of hepatectomy (major/minor)	20/18	42/62	0.28

Note: Data are presented as n or n/N, or median (IQR); between-group comparisons used the chi-square test, Fisher exact test, or Mann-Whitney U test. CEA, carcinoembryonic antigen; IQR, interquartile range; RAS/BRAF, rat sarcoma viral oncogene homolog / v-raf murine sarcoma viral oncogene homolog B.

Table 2: Spatial infiltration density of TAM subsets (cells/mm2, mean +- SD)

TAM subset	Tumor center (TC)	Invasive margin (IM)	Peritumoral region (PT)	P (IM vs TC)	P (PT vs TC)
CD68+	186 +- 52	312 +- 87	274 +- 71	<0.001	<0.001
CD163+	142 +- 43	248 +- 76	285 +- 82	<0.001	<0.001
CD80+	38 +- 15	52 +- 21	61 +- 24	0.004	0.002
SPP1+	64 +- 28	156 +- 54	98 +- 37	<0.001	<0.001
HLA-DRB5+	52 +- 22	78 +- 31	95 +- 38	0.007	<0.001
TREM2+ (exploratory, n=68)	71 +- 33	138 +- 48	82 +- 35	<0.001	0.21

Note: Data are presented as mean +- SD, in cells/mm2; TC, tumor center; IM, invasive margin; PT, peritumoral region; between-group comparisons used the paired t-test or Wilcoxon signed-rank test.

Table 3: Multivariable Cox regression: independent factors for postoperative RFS (limited to 4 variables, EPV constraint)

Variable	HR (95% CI)	P value
SPP1+ TAM IM (per +1 SD)	1.78 (1.16-2.73)	0.004
CD80/CD163 ratio PT (per +1 SD)	0.62 (0.43-0.89)	0.011
Number of metastases (>=4 vs 1-3)	1.74 (1.09-2.78)	0.019
N stage (N2 vs N0-N1)	1.58 (1.02-2.45)	0.041

Note: HR, hazard ratio; CI, confidence interval; SD, standard deviation; SPP1+ TAM@IM denotes invasive-margin SPP1+ TAM density; CD80/CD163@PT denotes the peritumoral CD80/CD163 ratio. Preoperative chemotherapy, RAS/BRAF mutation, age, and preoperative CEA were not included in the primary multivariable model (EPV constraint); their univariable analyses were all P>0.05 (data not shown).

Table 4A: Performance of the recurrence prediction model

Metric	Value
C-index (bootstrap-corrected)	0.71 (0.64-0.78)
1-year RFS AUC	0.76 (0.68-0.84)
2-year RFS AUC	0.72 (0.63-0.81)
Calibration slope (2-year)	0.88

Table 4B: TAM-RRS risk stratification and postoperative RFS

TAM-RRS group	n	Median RFS (months)	2-year RFS rate	HR (vs low risk)
Low risk	68	32.4	61.8%	Reference
High risk	74	9.6	27.0%	2.63 (1.71-4.05)

Note: The cutoff was the overall median TAM-RRS; patients were not divided into arbitrary equal groups. TAM-RRS, TAM subset-based risk score; RFS, recurrence-free survival.

Table 4C: Incremental value of the model (delta C-index / NRI / IDI)

Model	C-index (95% CI)	delta C-index / NRI / IDI
Clinical model		Reference
Clinical + TAM model	0.71 (0.64-0.78)	

Table 5: Kaplan-Meier analysis of postoperative RFS by TAM subset group

Grouping criterion	n	Median RFS (months)	2-year RFS rate	HR (95% CI)	P value
SPP1+ IM high density (>=148)	74	11.2	63.5%	2.14 (1.37-3.34)	<0.001
SPP1+ IM low density (<148)	68	26.8	60.3%	Reference	-
CD80/CD163 PT high (>=0.28)	68	24.5	58.8%	0.55 (0.36-0.84)	0.006
CD80/CD163 PT low (<0.28)	74	13.6	35.1%	Reference	-
HLA-DRB5+ IM high density (>=78)	68	22.4	49.2%	0.72 (0.48-1.08)	0.11
HLA-DRB5+ IM low density (<78)	74	16.1	38.5%	Reference	-
TREM2+ IM high density (>=132) [exploratory]	35	9.8	25.7%	2.31 (1.28-4.16)	0.005
TREM2+ IM low density (<132) [exploratory]	33	23.6	54.5%	Reference	-

Note: Cutoffs were the overall median; HR is for the high-density group relative to the low-density group; KM, Kaplan-Meier; RFS, recurrence-free survival.

Table 6: TAM characteristics in early recurrence vs non-early recurrence

TAM parameter	Early recurrence (n=38)	Non-early recurrence (n=104)	P value
SPP1+ TAM IM density (cells/mm2)	182 +- 61	146 +- 54	<0.001
TREM2+ TAM IM density (n=68)	156 +- 52	112 +- 44	0.004
CD163+ TAM PT density (cells/mm2)	248 +- 76	299 +- 88	0.008
CD80/CD163 ratio PT	0.21 +- 0.09	0.29 +- 0.12	0.006
HLA-DRB5+ TAM IM density (cells/mm2)	64 +- 28	83 +- 36	0.002

Note: Data are presented as mean +- SD; IM, invasive margin; PT, peritumoral region.

Supplementary Table S1: Effect of preoperative chemotherapy on TAM subset infiltration

TAM subset	Preoperative chemotherapy (n=86)	No chemotherapy (n=56)	P value
CD68+ (IM)	268 +- 79	342 +- 91	0.006
CD163+ (IM)	204 +- 68	285 +- 82	<0.001
CD80+ (IM)	49 +- 19	56 +- 23	0.23
SPP1+ (IM)	142 +- 51	168 +- 58	0.14
HLA-DRB5+ (IM)	72 +- 29	84 +- 34	0.09

Supplementary Table S2: Validation using public single-cell data

TAM subset	Proportion in CRLM (%)	Proportion in primary tumor (%)	P value
SPP1+ TAM	18.4	8.2	<0.001
HLA-DRB5+ TAM	12.1	15.6	0.03
TREM2+ TAM	9.8	4.1	<0.001

References

[1] paradigms and future directions. Cell Mol Gastroenterol Hepatol, 2017, 3(2): 163-173.
[2] VIGANO L, GENTILE D, GALVANIN J, et al. Very early recurrence after liver resection for colorectal metastases: incidence, risk factors, and prognostic impact. J Gastrointest Surg, 2022, 26(3): 570-582.
[3] YAMASHITA Y, ADACHI E, TOH Y, et al. Risk factors for early recurrence after curative hepatectomy for colorectal liver metastases. SurZAROUR L R, ANAND S, BILLINGSLEY K G, et al. Colorectal cancer liver metastasis: evolving g Today, 2011, 41(4): 526-532.
[4] INOUE Y, FUJII K, KAGOTA S, et al. The management of recurrence within six months after hepatic resection for colorectal liver metastasis. Dig Surg, 2020, 37(4): 282-291.
[5] FREIRE VALLS A, KNIPPER K, GIANNAKOURI E, et al. VEGFR1(+) metastasis-associated macrophages contribute to metastatic angiogenesis and influence colorectal cancer patient outcome. Clin Cancer Res, 2019, 25(18): 5674-5685.
[6] ZHAO S, MI Y, GUAN B, et al. Tumor-derived exosomal miR-934 induces macrophage M2 polarization to promote liver metastasis of colorectal cancer. J Hematol Oncol, 2020, 13(1): 156.
[7] PAVLOV S, ALI E, AMBROZKIEWICZ F, et al. Macrophages in colorectal cancer: from normal mucosa to distant metastasis: beyond the M1/M2 paradigm. J Cancer, 2026, 17(1): 157-176.
[8] HUANG M, YUAN J X. Mechanisms and research progress of M1/M2 macrophage polarization in colorectal cancer liver metastasis. Chin J Diff Compl Cas, 2026, 25(9): 1140-1145.
[9] WU Y, YANG S, MA J, et al. Spatiotemporal immune landscape of colorectal cancer liver metastasis at single-cell level. Cancer Discov, 2022, 12(1): 134-153.
[10] BILL R, WIRAPATI P, MESSEMAKER M, et al. CXCL9:SPP1 macrophage polarity identifies a network of cellular programs that control human cancers. Science, 2023, 381(6657): 515-524.
[11] MOLGORA M, LIU Y A, COLONNA M, et al. TREM2: a new player in the tumor microenvironment. Semin Immunol, 2023, 67: 101739.
[12] LONG Y X, ZHANG H M. Distribution, function and clinical significance of SPP1+ macrophages in colorectal cancer. Chin J Clin Oncol, 2025, 52(12): 633-637.
[13] LIU Y, ZHANG Q, XING B, et al. Immune phenotypic linkage between colorectal cancer and liver metastasis. Cancer Cell, 2022, 40(4): 424-437.e5.
[14] DING D, LI W, REN J, et al. SPP1(high) macrophage-induced T-cell stress promotes colon cancer liver metastasis through SPP1/CD44/PI3K/AKT signaling. J Immunother Cancer, 2025, 13(10): e012330.
[15] CHANG M, FENG M, LEI Y, et al. Integrated single-cell and spatial transcriptomic analysis reveals mCAF-SPP1 macrophage-T cell crosstalk shaping immunosuppressive niches in colorectal cancer liver metastasis. J Transl Med, 2026, 24(1): 168.
[16] CHE L H, LIU J W, HUO J P, et al. A single-cell atlas of liver metastases of colorectal cancer reveals reprogramming of the tumor microenvironment in response to preoperative chemotherapy. Cell Discov, 2021, 7(1): 80.
[17] ZHU X X, LONG Z, CAO S H. M2 tumor-associated macrophages in colorectal cancer tissue predict the risk of lymph node metastasis. Chin J Clin Res, 2024, 37(9): 1369-1373.
[18] KHANDURI I, MAKI H, VERMA A, et al. New insights into macrophage polarization and its prognostic role in patients with colorectal cancer liver metastasis. BJC Rep, 2024, 2(1): 37.
[19] ZHENG X, WEIGERT A, REU S, et al. Spatial density and distribution of tumor-associated macrophages predict survival in non-small cell lung carcinoma. Cancer Res, 2020, 80(20): 4414-4425.
[20] YANG D, SUN X, WANG H, et al. TREM2 depletion in pancreatic cancer elicits pathogenic inflammation and accelerates tumor progression via enriching IL-1beta(+) macrophages. Gastroenterology, 2025, 168(6): 1153-1169.